AN INVESTIGATION OF THE AEROELASTIC STABILITY OF THIN CYLINDRICAL SHELLS AT TRANSONIC MACH NUMBERS

T. M. Perkins and T. R. Brice
ARO, Inc.

May 1966

PROPULSION WIND TUNNEL FACILITY
ARNOLD ENGINEERING DEVELOPMENT CENTER
AIR FORCE SYSTEMS COMMAND
ARNOLD AIR FORCE STATION, TENNESSEE

NOTICES

AN INVESTIGATION OF THE AEROELASTIC STABILITY OF THIN CYLINDRICAL SHELLS AT TRANSONIC MACH NUMBERS

T. M. Perkins and T. R. Brice
ARO, Inc.

AF - AEDC
Arnold AFS Tenn

FOREWORD

The work reported herein was done at the request of the Air Force Office of Scientific Research (AFOSR), Air Force Systems Command (AFSC), Aeronautical Research Laboratory (ARL), and Midwest Research Institute (MRI), under Program Element 61445014, Project 7063.

The results of the tests presented were obtained by ARO, Inc. (a subsidiary of Sverdrup & Parcel and Associates, Inc.), contract operator of the Arnold Engineering Development Center (AEDC), AFSC, Arnold Air Force Station, Tennessee, under Contract AF40(600)-1200. The tests were conducted from December 27, 1965, through January 10, 1966, under ARO Project No. PB0504, and the manuscript was submitted for publication on April 6, 1966.

This technical report has been reviewed and is approved.

Francis M. Williams
Major, USAF
AF Representative, PWT
DCS/Test

Jean A. Jack
Colonel, USAF
DCS/Test

ABSTRACT

Static pressure and boundary-layer data were obtained over a rigid pressure shell at Mach numbers from 1.20 to 1.50 and Reynolds numbers from 1.04 to 4.20 x 10^6/ft in the 16-ft transonic tunnel. These data were obtained with and without addition of air into the boundary layer through a circular slot upstream of the test shell. Flutter characteristics of thin cylindrical shells were obtained at Mach numbers of 1.20 and 1.50 with and without boundary-layer blowing and shell axial loading. Spirally traveling waves appeared on three of the shells just prior to divergent flutter, which was initiated by reducing shell cavity pressure.

CONTENTS

ILLUSTRATIONS

TABLE

NOMENCLATURE

BLC	Boundary-layer control valve position, percent open
C_p	Pressure coefficient, $\frac{p - p_\infty}{q_\infty}$
E	Young's modulus of elasticity, 16×10^6 psi
$\overline{F}$	Flutter parameter, $\left(\frac{q_\infty}{E\sqrt{M_\infty^2 - 1}}\right)^{1/3} \cdot R/h$
f	Shell flutter frequency, cps
h	Shell thickness, in.
L	Length of pressure shell, in.

M_∞	Free-stream Mach number
n	Wave speed, in./sec
p	Local pressure on model surface, psf
p_a	Pressure in axial bladder, psi
p_c	Shell cavity pressure, psi
p_r	Pressure in radial bladder, psi
p_{t_∞}	Free-stream total pressure, psf
p_∞	Free-stream static pressure, psf
q_∞	Free-stream dynamic pressure, psf
R	Model radius, 8 in.
Re/ft	Reynolds number per foot
T_{t_a}	Tunnel total temperature, °F
t	Time, sec
U_∞	Free-stream velocity, ft/sec
u	Local velocity, ft/sec
$\dot{w}$	Weight flow in BLC duct, lb/sec
x	Distance from forward edge of shell to individual orifice, in.
y	Vertical distance above model surface, in.
Δp_c	Differential pressure across test shell, $(p_c - p_\infty)$, psi

SECTION I
INTRODUCTION

An investigation into the aeroelastic stability of thin cylindrical shells was conducted in the Propulsion Wind Tunnel, Transonic (16T). The test was divided into a pressure phase and a flutter phase.

The purpose of the pressure phase was to determine boundary-layer profiles and static pressure distributions over a rigid shell with and without addition of air into the boundary layer for Mach numbers from 1.20 to 1.50 at two Reynolds number levels.

The objective of the flutter phase was to determine the flutter characteristics of five flexible cylindrical shells as influenced by shell thickness, boundary-layer thickness, shell cavity pressure, and shell axial loading at Mach numbers 1.20 and 1.50.

SECTION II
APPARATUS

2.1 WIND TUNNEL

Tunnel 16T is a continuous flow, closed-circuit wind tunnel capable of operating from a stagnation pressure level of 60 to 5000 psf. The test section is 16 ft square by 40 ft long with perforated walls to allow continuous operation through the Mach number range from 0.5 to 1.6 with minimum wall interference.

Details of the perforated walls and the location of the model and support strut in the test section are shown in Fig. 1. A photograph of the model installed in Tunnel 16T is presented in Fig. 2.

2.2 TEST ARTICLE

A detailed drawing of the ogive-cylinder model is shown in Fig. 3. The model has a 3-cal circular arc ogive nose with an 18.9-deg semivertex angle, a fineness ratio of approximately 8, and a maximum diameter of 16 in. It is composed of three basic sections: the nose cone, center section, and the aft or base supporting structure. The primary function of the nose cone is to provide a uniform flow and static pressure

field over the test shell and to support the boundary-layer control equipment. The center section supports either the pressure shell or thin flutter shell and its associated instrumentation, whereas the base section attaches the model to the supporting sting.

Details of the pressure and flutter shells are presented in Figs. 4a and b. The static pressure shell was constructed from 0.080-in. copper sheet with four rows of orifices along the shell. Additional orifices were located on the model as shown in Fig. 3. Two boundary-layer rakes, one fixed and one remotely adjustable, were located at model station 114.25. The fixed and adjustable rakes are illustrated in Figs. 5 and 6, respectively.

The flutter shells were thin-walled monocoque circular cylinders made by an electroplating process which is outlined in Ref. 1. The shell thicknesses were 0.0020, 0.0032, and 0.0040 in., as shown in Table I. These shells were soldered to two copper end rings which were machined to fit smoothly against radial and axial bladders. These bladders were located inside the fore and aft edges of the center section. The internal pressure in the axial bladders could be remotely controlled to produce an axial buckling load (longitudinally compressive) in the shell. Figure 7 shows a calibration curve for axial load versus axial bladder pressure for one value of shell cavity pressure. Figure 8 is a photograph of the 0.0032-in. shell buckled by an axial load of 240 lb with zero cavity pressure differential. The characteristic diamond patterns in the shell will be evident in the flutter photographs which are discussed in Section IV.

2.3 INSTRUMENTATION

2.3.1 Pressure Phase

Twenty-four static pressure orifices were uniformly distributed along four rays on the shell, and nine orifices were located elsewhere on the model as shown in Fig. 3. Three static pressure orifices were located internally in the boundary-layer control duct, and one orifice was installed in the cavity beneath the pressure shell. All the pressure orifices were connected to pressure transducers which were located in the tunnel plenum chamber. All transducer outputs were fed to analog-to-digital converters and then to a digital computer.

Two boundary-layer rakes were used to measure the boundary-layer thickness over the shell. The fixed rake had ten total pressure orifices, and the remotely adjustable rake had one static and six total pressure

orifices connected to transducers with the outputs introduced into the computer in the same manner as the pressure orifices in the shell.

2.3.2 Flutter Phase

A photograph of the model instrumentation used in the flutter phase is presented in Fig. 9. The model displacement sensors were mutual-inductance proximity transducers and were designed to sense both static and dynamic displacements of a point on the shell surface without mechanical contact (Ref. 1). Sensor 1 could translate fore and aft from 10 to 85 percent of the shell length at a speed of 25 in./min. Both sensors 1 and 2 could rotate circumferentially under the shell from 0 through 270 deg. Sensor 3, which is covered in the photograph, was fixed in position and used as a reference sensor to assist in mode shape identification through phase-angle measurements between this sensor and the two moving sensors.

The signals from these sensors were amplified and fed into two magnetic tape recorders and a direct-writing oscillograph as shown in Fig. 10. A dual-beam oscilloscope was used for continuous monitoring of shell motion. The input to this scope could be varied from one sensor to another as it became necessary to compare the phasing and relative amplitude of the three sensors. The magnetic tape recorders were sometimes run continuously when the shell signals appeared to coalesce in frequency and increase in amplitude.

SECTION III
TEST PROCEDURES

3.1 PRESSURE PHASE

Boundary-layer profiles and static pressure distributions were obtained at Mach numbers from 1.20 to 1.50 at Reynolds numbers of approximately 1.04 and 4.20 x 10^6/ft (Fig. 11). Air was blown into the boundary layer through a circumferential slot ahead of the test shell at M_∞ = 1.20 and 1.50 for both Reynolds number levels.

The Mach numbers were obtained by means of the flexible nozzle plates using plenum pressure control to stabilize the flow through the test section. The desired Reynolds numbers were obtained by establishing the proper stagnation pressure and temperature. A test section wall angle setting of zero was maintained throughout the pressure phase of this test.

The boundary-layer control (BLC) system was operated at valve positions of 0 and 25 percent open. A maximum weight flow of 0.36 lb/sec was obtained from the 0.064-in. circumferential slot for a valve setting of 25 percent open. All BLC data shown are for either zero weight flow or for the maximum of 0.36 lb/sec.

3.2 FLUTTER PHASE

For the five flexible shell configurations tested, the Mach number was established at 1.20 and 1.50 with a low dynamic pressure. The dynamic pressure was then slowly increased in steps at constant Mach number until tunnel maximum or a designated limit was obtained. After desired total pressure level was reached, model cavity pressure was reduced until flutter occurred. Mass addition of air into the boundary layer, internal pressure, and shell axial loading were varied only when tunnel conditions were constant.

3.3 PRECISION OF MEASUREMENTS

The magnitude of the uncertainties involved in the tunnel conditions is estimated to be as follows:

Mach Number	±0.005
Total Pressure	±5 psf
Dynamic Pressure	±0.5 percent
Total Temperature	±5°F

The Mach number error does not include the deviation from the mean value in the region of the model. The maximum variation in Mach number on the tunnel centerline between the tunnel stations by the model was ±0.007.

The magnitude of the uncertainties in shell frequency measurement, based on repeatability during the wind-off calibrations, and the accuracies in determining shell flutter frequencies from oscillograph records of the variable inductance sensors are estimated to be 2 cps.

SECTION IV
RESULTS AND DISCUSSION

4.1 PRESSURE PHASE

The boundary-layer distributions were measured with a fixed and an adjustable rake at model station 114.25. Only the fixed rake data are

presented since vertical positioning difficulties were encountered with the remotely adjustable rake. These boundary-layer profiles are presented in Fig. 12a for Mach numbers from 1.20 to 1.50 for two Reynolds number levels. Boundary-layer profiles were also obtained with and without mass addition of air into the boundary layer at M_∞ = 1.20 and 1.50 for both Reynolds number levels as shown in Fig. 12b.

Boundary-layer displacement and momentum thicknesses were computed from the profile data. Both the displacement and momentum thicknesses increased with increasing Mach number and decreased with increasing Reynolds number as expected from the theory of turbulent flow over flat plates (Ref. 2).

Insignificant changes in the boundary-layer profiles resulted from mass additions of air into the boundary layer. It is believed that larger values of weight flow would be required to produce a significant change in the boundary-layer characteristics.

The variation in pressure coefficient (C_p) with x/L at Mach numbers from 1.20 to 1.50 is presented in Fig. 13. The maximum variation in the pressure coefficient across the shell was from -0.043 to +0.032 along the 180-deg ray at M_∞ = 1.20.

4.2 FLUTTER PHASE

Five shell configurations were tested, three at M_∞ = 1.20 and two at M_∞ = 1.50. A summary of the test results and initial conditions is presented in Table I.

Configuration 1 experienced a divergent flutter mode as the shell cavity pressure was being slowly reduced to 0.236 psi. The shell buckled inward against the center section, then outward, and fluttered violently to destruction. The flutter frequency was higher for this failure than for any of the other shell failures, which indicated a different mode of flutter caused by the floating end-fixity and low cavity pressure. The mode of flutter appeared to be that of "shell breathing" as viewed on closed-circuit television.

Configuration 2 was loaded axially to 124 lb, which represented the wind-off axial buckling load with a positive cavity pressure differential of 1 psi. After the tunnel conditions were stabilized and no significant shell motions were noted, the BLC valve was opened to the 25-percent position at which point divergent flutter occurred before high speed motion pictures could be obtained.

The ends were fixed in configuration 3 in an attempt to prevent complete loss of the shell. The internal cavity pressure differential was rapidly reduced from 1 psi (positive) to initiate shell flutter as high speed motion pictures were being obtained. When Δp_c equalled 0.754 psi, a longitudinal traveling wave mode of flutter was triggered. This traveling wave is shown in Fig. 14a. The longitudinal traveling wave became more of a spirally traveling wave after approximately 0.27 sec as shown in Fig. 14b. The occurrence of flutter from start to failure required approximately 0.32 sec.

The oscillograph trace presented in Fig. 15 shows the divergent flutter encountered during the testing of configuration 4, which was geometrically identical to configuration 2. For configuration 4, the BLC was zero, and the shell cavity pressure (Δp_c) was rapidly reduced from 1.0 to 0.440 psi before shell flutter began. High speed motion pictures of this shell failure indicated a more spirally traveling wave mode of flutter than that of configuration 3.

Configuration 5 was axially loaded to its wind-off buckling load of 210 lb for Δp_c initially equal to 1 psi. The shell cavity pressure was reduced until flutter was initiated. It appears that the airstream is somewhat stabilizing to shell buckling since no local deformation or waves were formed until Δp_c was reduced to 0.530 psi.

The average value of the flutter parameter ($\overline{F}$) from Table I is 23.6 for the present investigation. The average value of $\overline{F}$ is 7.0 in Ref. 3, which covered Mach numbers from 2.487 to 3.527. The flutter modes obtained in Ref. 3 were composed of circumferential waves having many nodal lines parallel to the model centerline. This flutter mode was not divergent because no shell failures were encountered.

The boundary-layer blowing data are not conclusive since only one point was obtained, but intuitive reasoning would indicate that reducing the boundary-layer displacement thickness would make the shell less stable.

SECTION V
CONCLUSIONS

The following conclusions were derived from this test:

5.1 PRESSURE PHASE

Blowing 0.36 lb of air per sec into the boundary layer produced no significant changes in the boundary-layer profiles at $M_\infty = 1.20$ and 1.50 for a Reynolds number per foot of 4.20×10^6.

5.2 FLUTTER PHASE

1. Decreasing shell cavity pressure initiated a destructive flutter mode at the Mach numbers of the investigation.
2. Destructive shell flutter was more violent when the shells were loaded axially. However, shell buckling caused by compressive axial loading appeared to be suppressed by the airstream.
3. The flutter modes appeared to be influenced by end-fixity. A "breathing mode" occurred when the shell was simply supported, and traveling wave modes occurred with either forward or both ends fixed. The spirally traveling wave was more evident when only the forward end of the shell was fixed.

REFERENCES

1. Olson, Mervyn D. "Supersonic Flutter of Circular Cylindrical Shells Subjected to Internal Pressure and Axial Compression." AROSR 65-0599, California Institute of Technology, April 1965.
2. Liepmann, H. W. and Roshko, A. Elements of Gas Dynamics. John Wiley and Sons, New York, 1957, pp. 340-342.
3. Stearman, R. O., Lock, M. H., and Fung, Y. C. "Ames Tests on the Flutter of Cylindrical Shells." SM62-37, California Institute of Technology, December 1962.

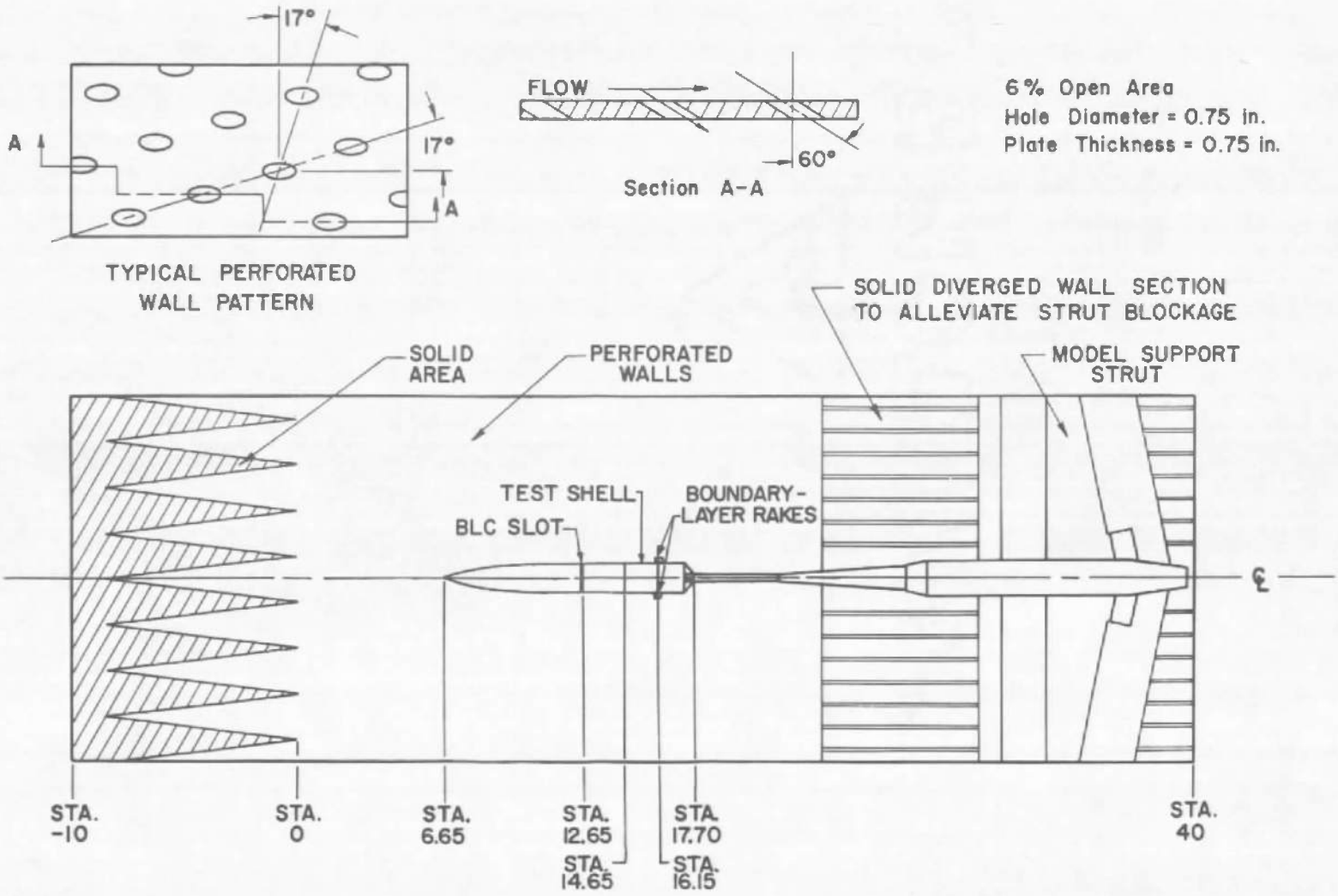

Fig. 1 Schematic of Tunnel 16T Test Section Showing Model Location

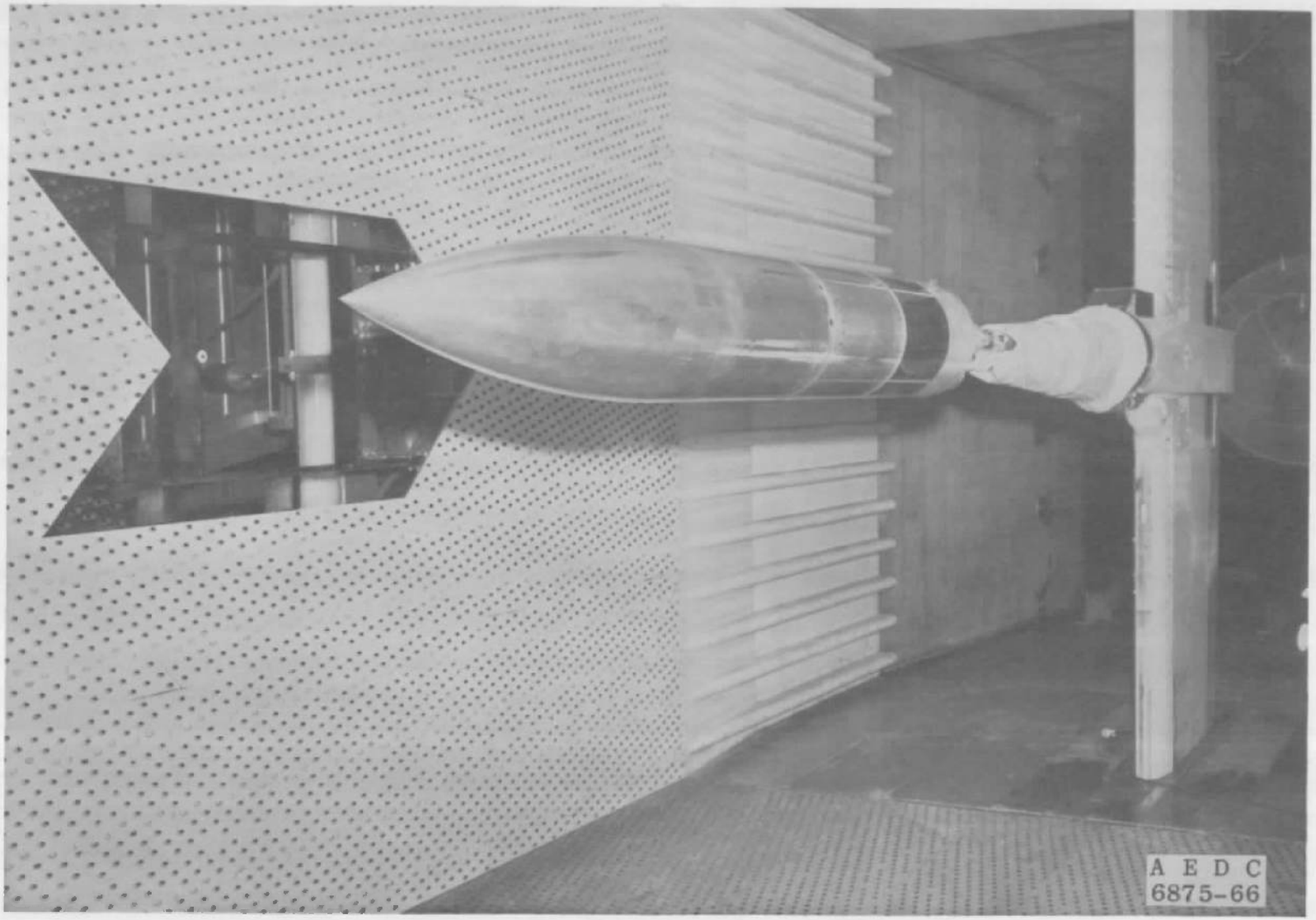

Fig. 2 Photograph of Ogive-Cylinder Model Installed in Tunnel 16T

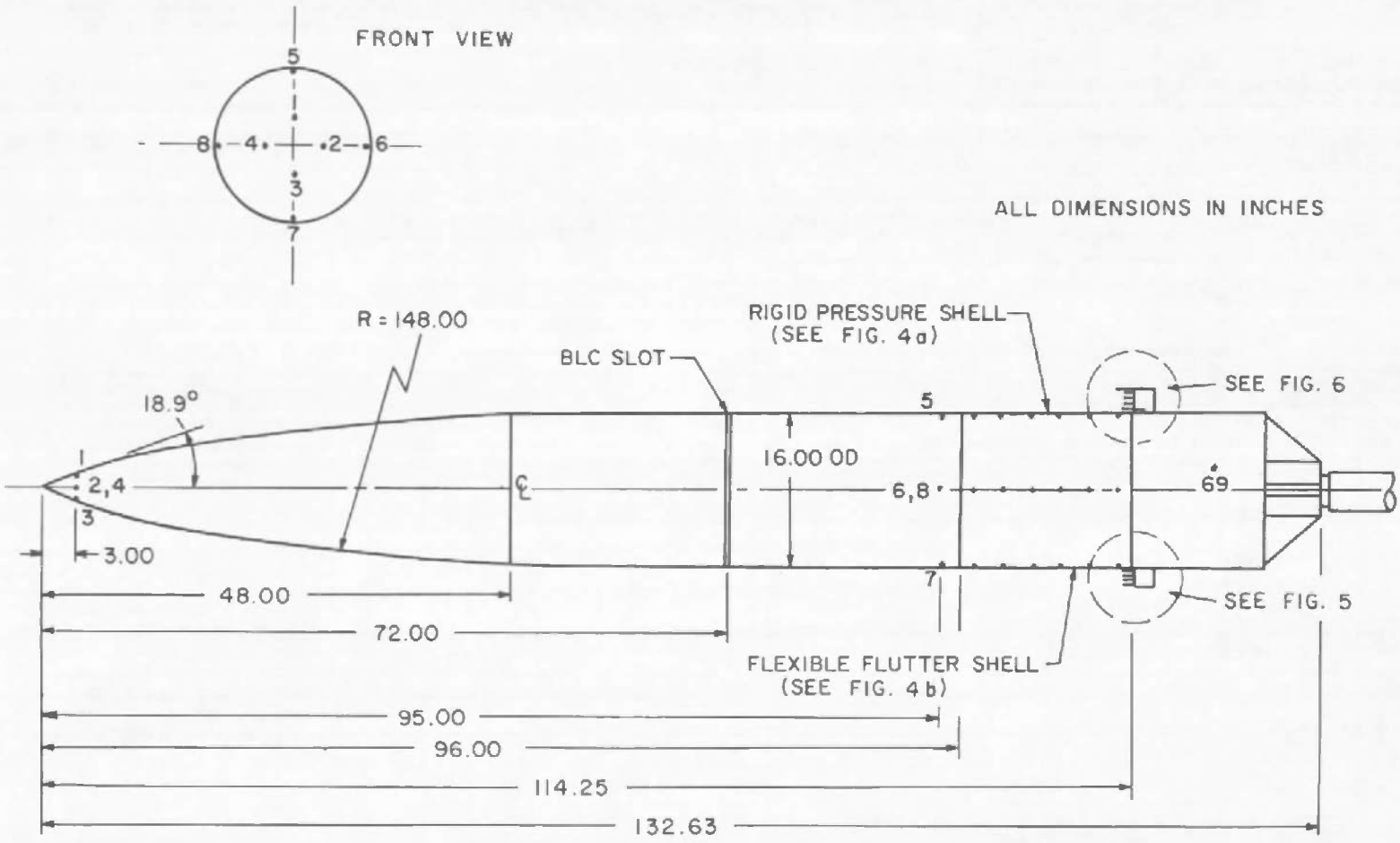

Fig. 3 Details of Ogive-Cylinder Model

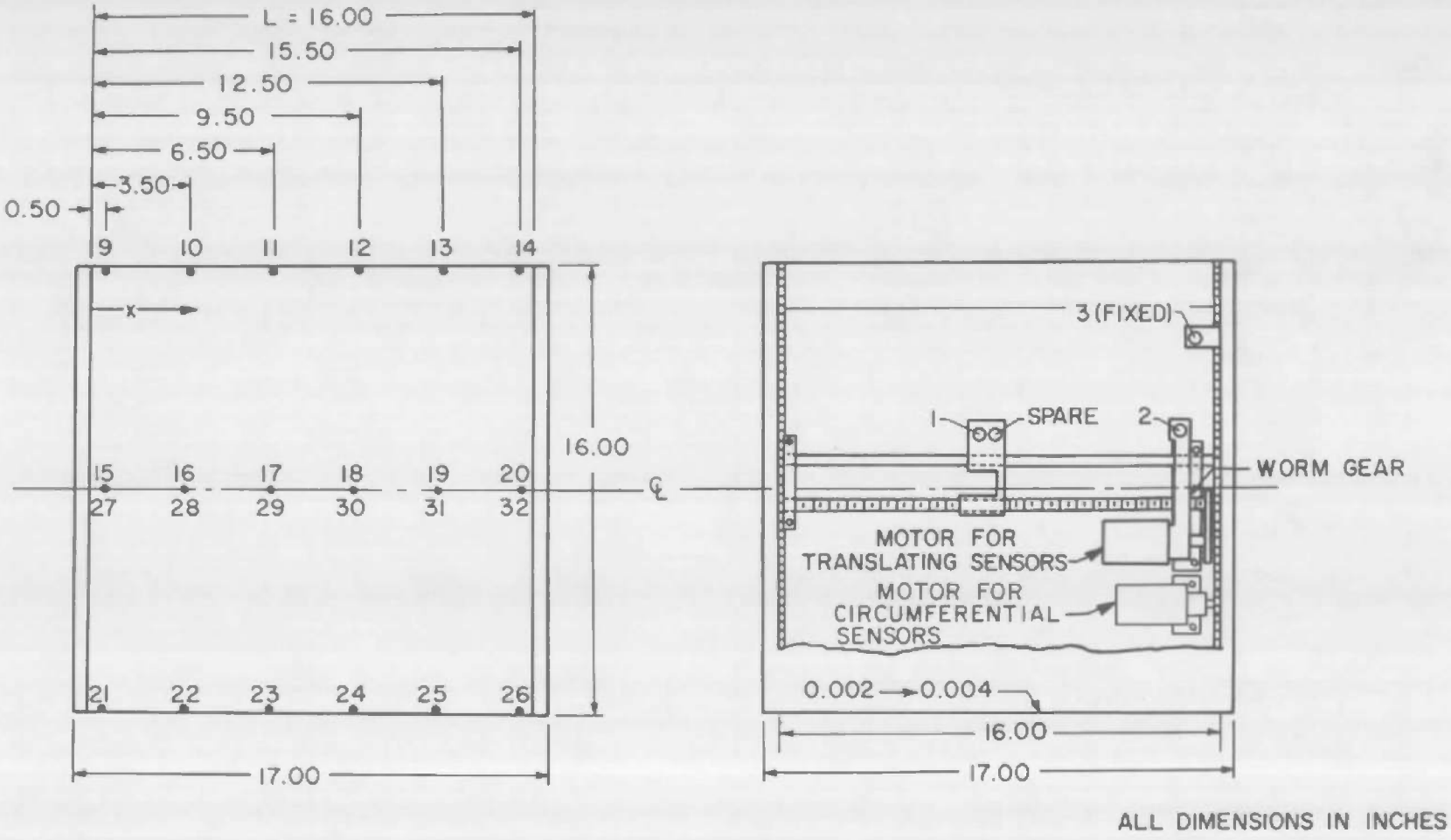

a. Rigid Pressure Shell

b. Flexible Flutter Shell

Fig. 4 Details of Test Shells

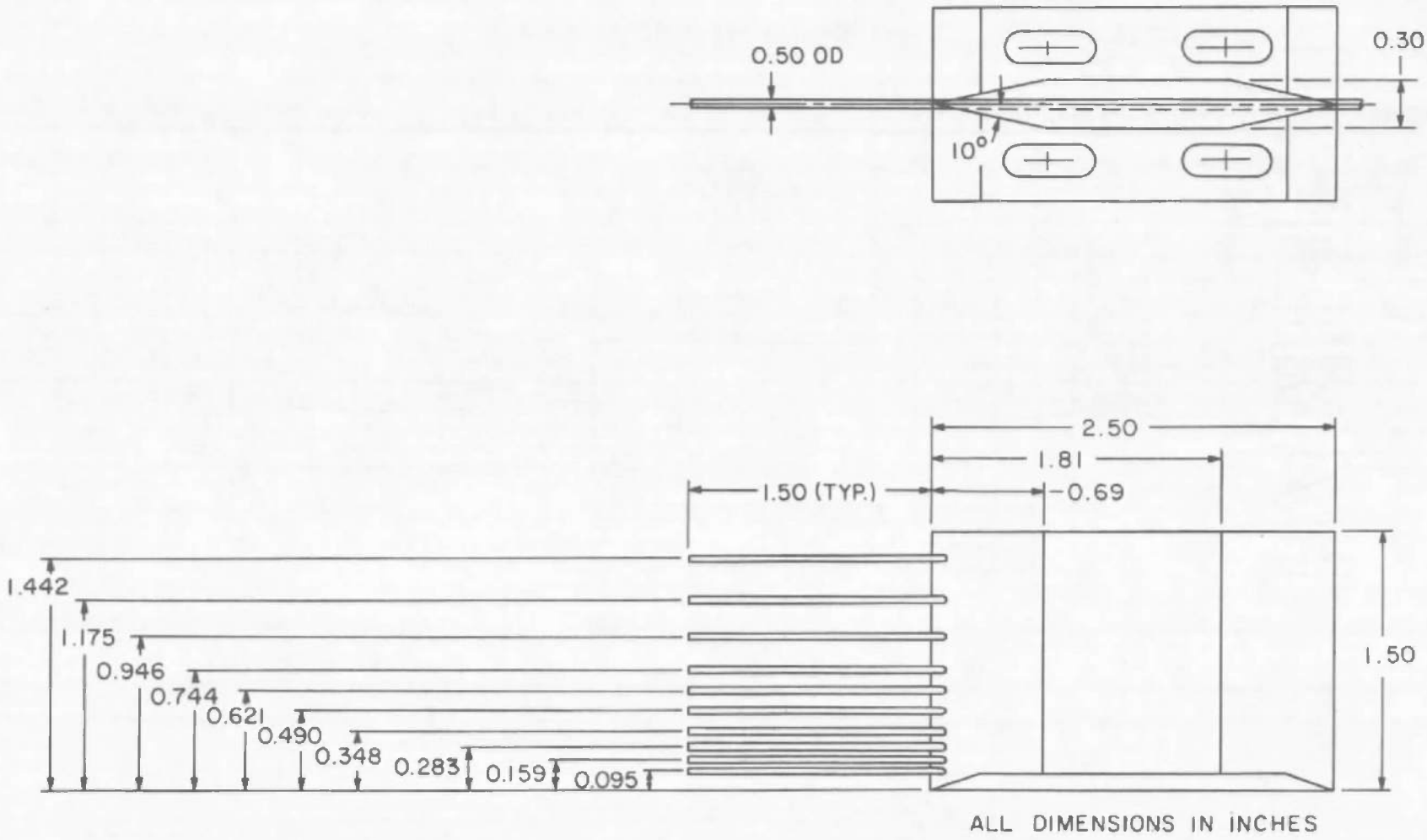

Fig. 5 Fixed Boundary-Layer Rake

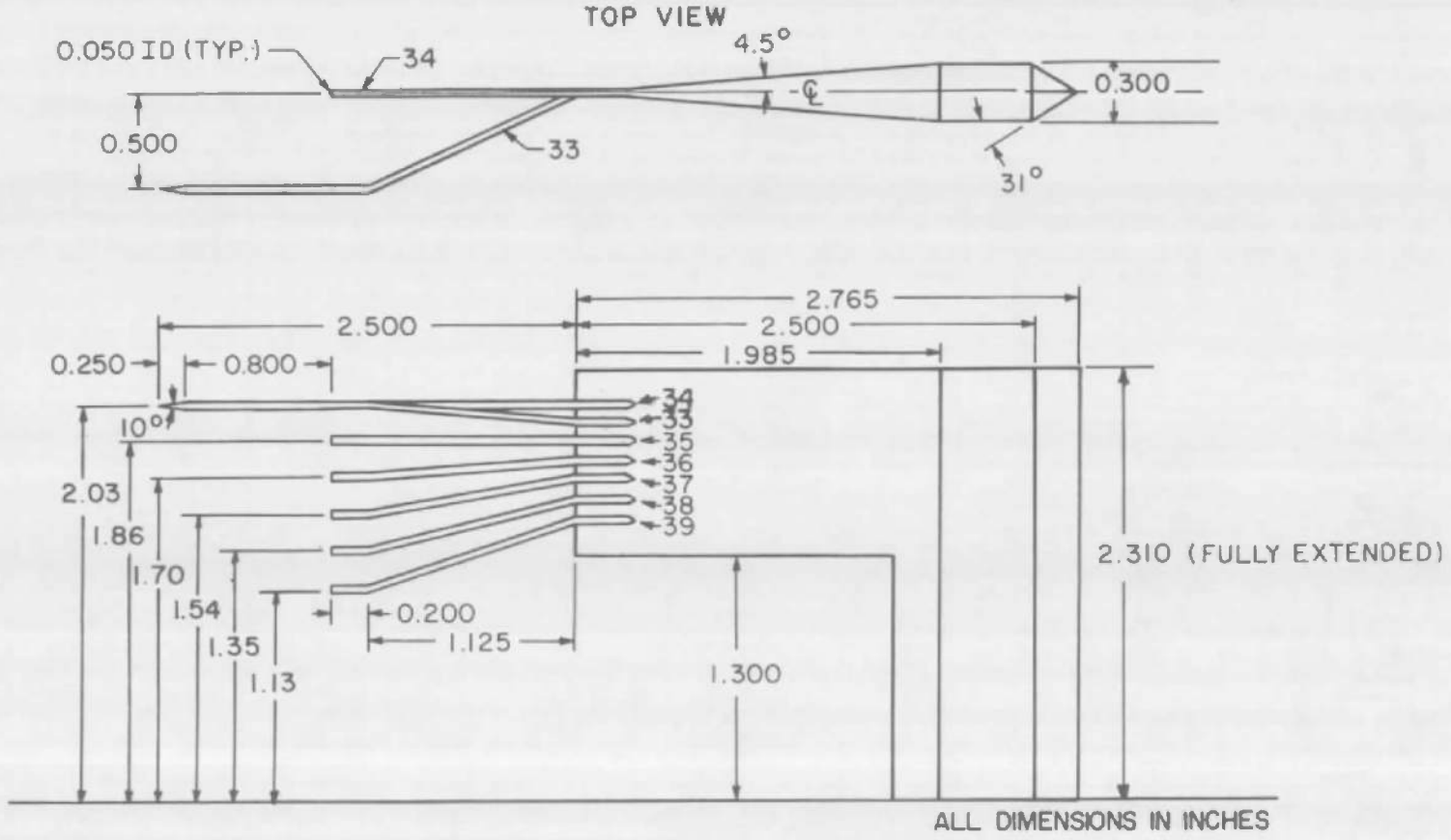

Fig. 6 Adjustable Boundary-Layer Rake

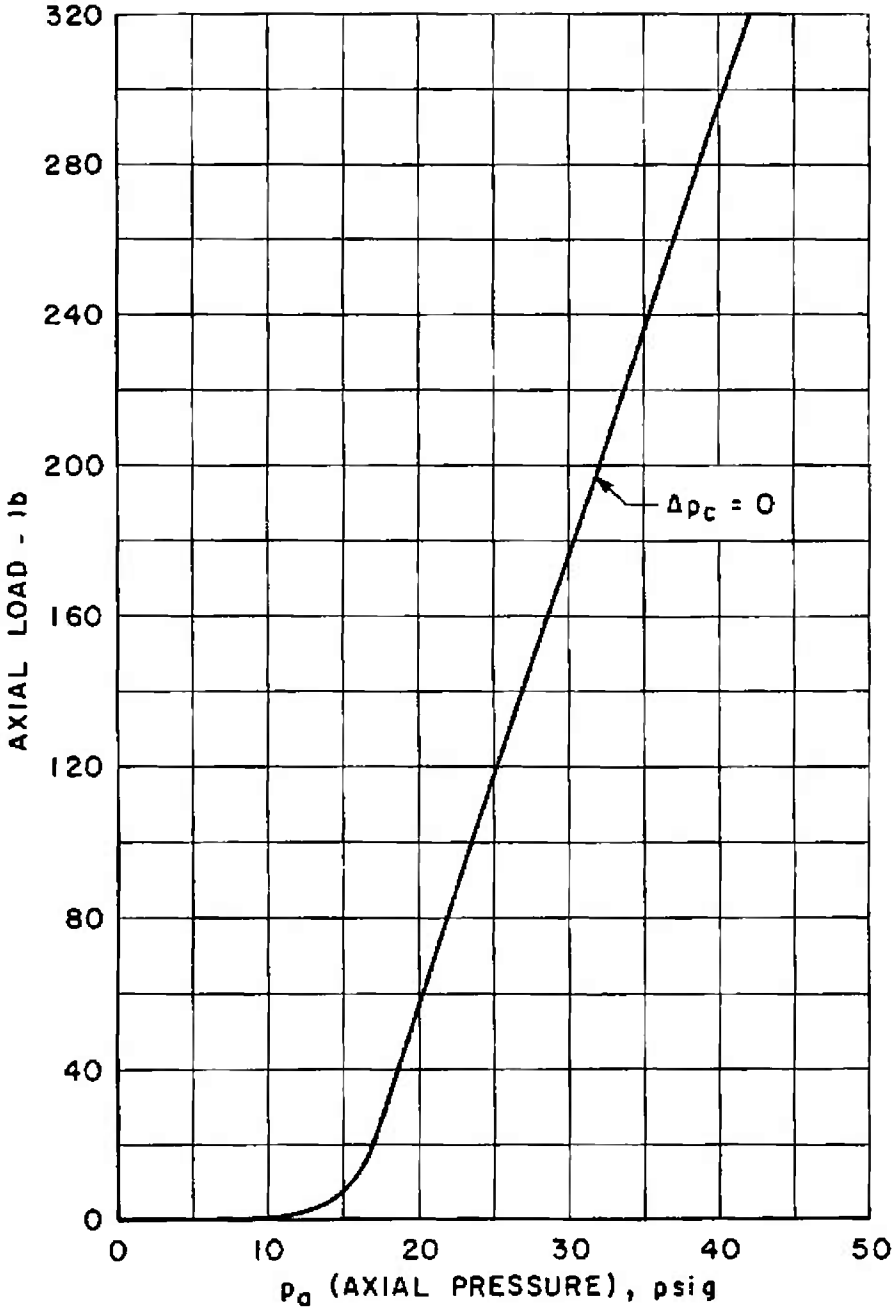

Fig. 7 Calibration Curve for Axial Bladders

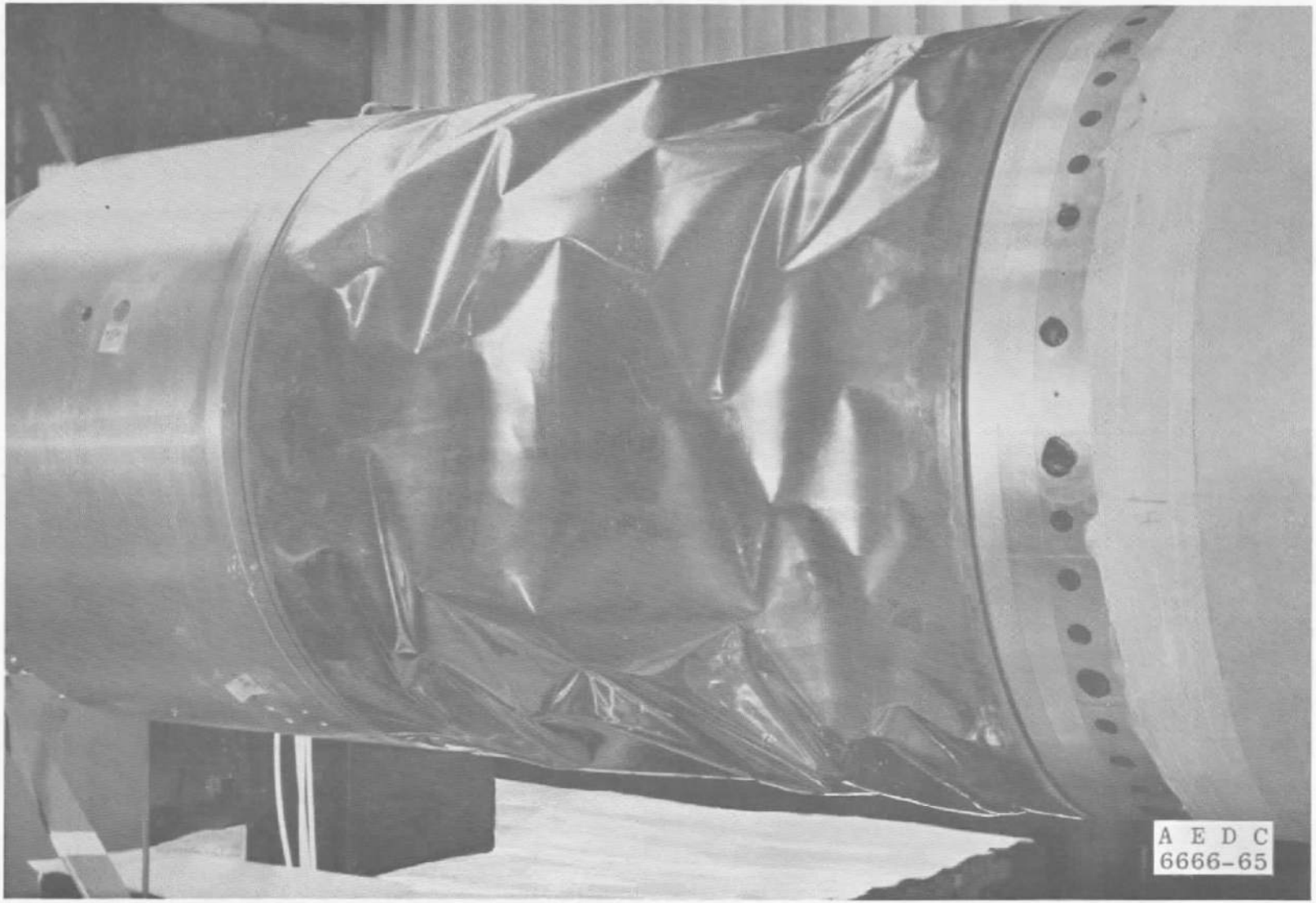

Fig. 8 Static Buckling of 0.0032-in. Flutter Shell

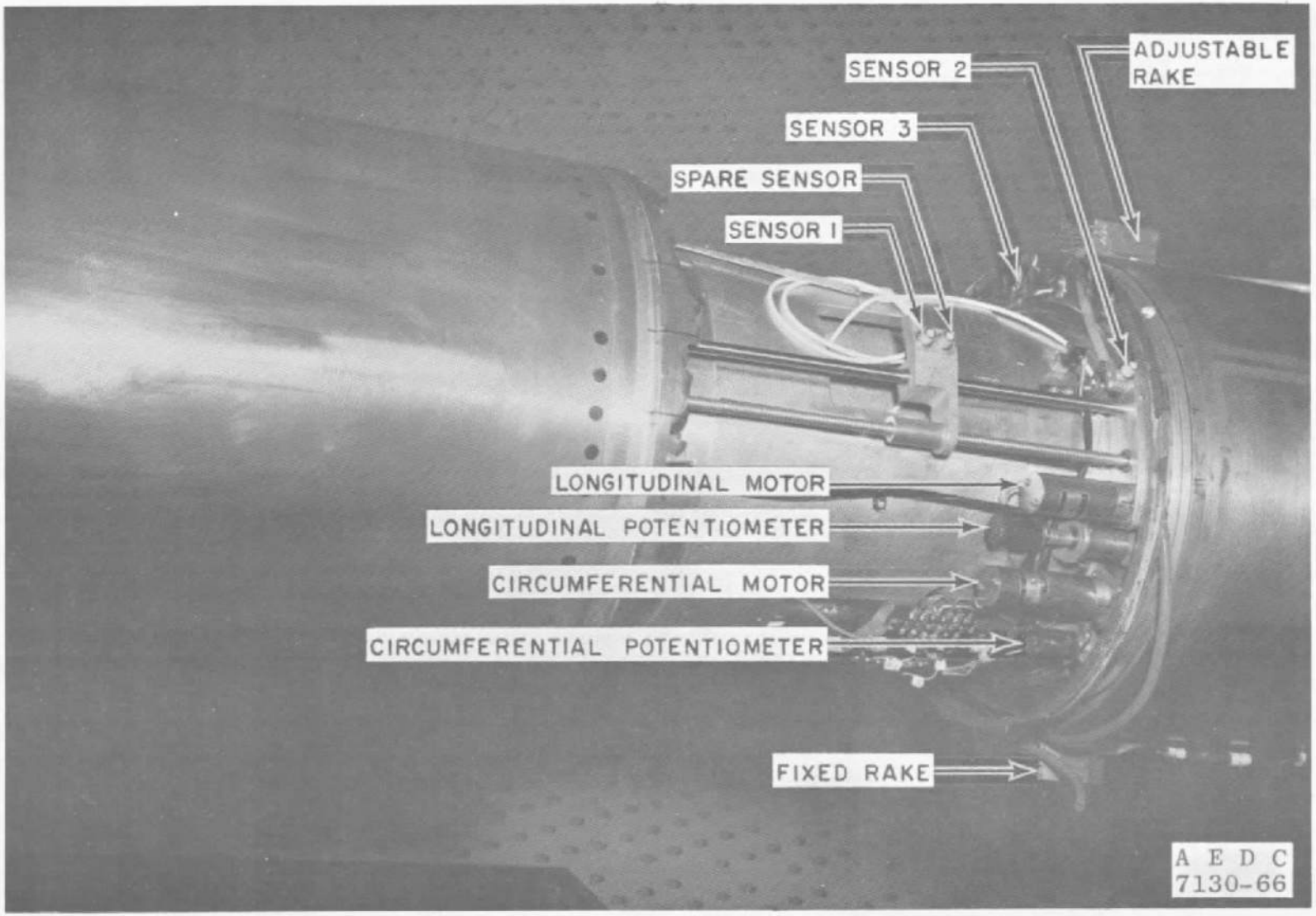

Fig. 9 Photograph of Model Instrumentation Used during Flutter Phase

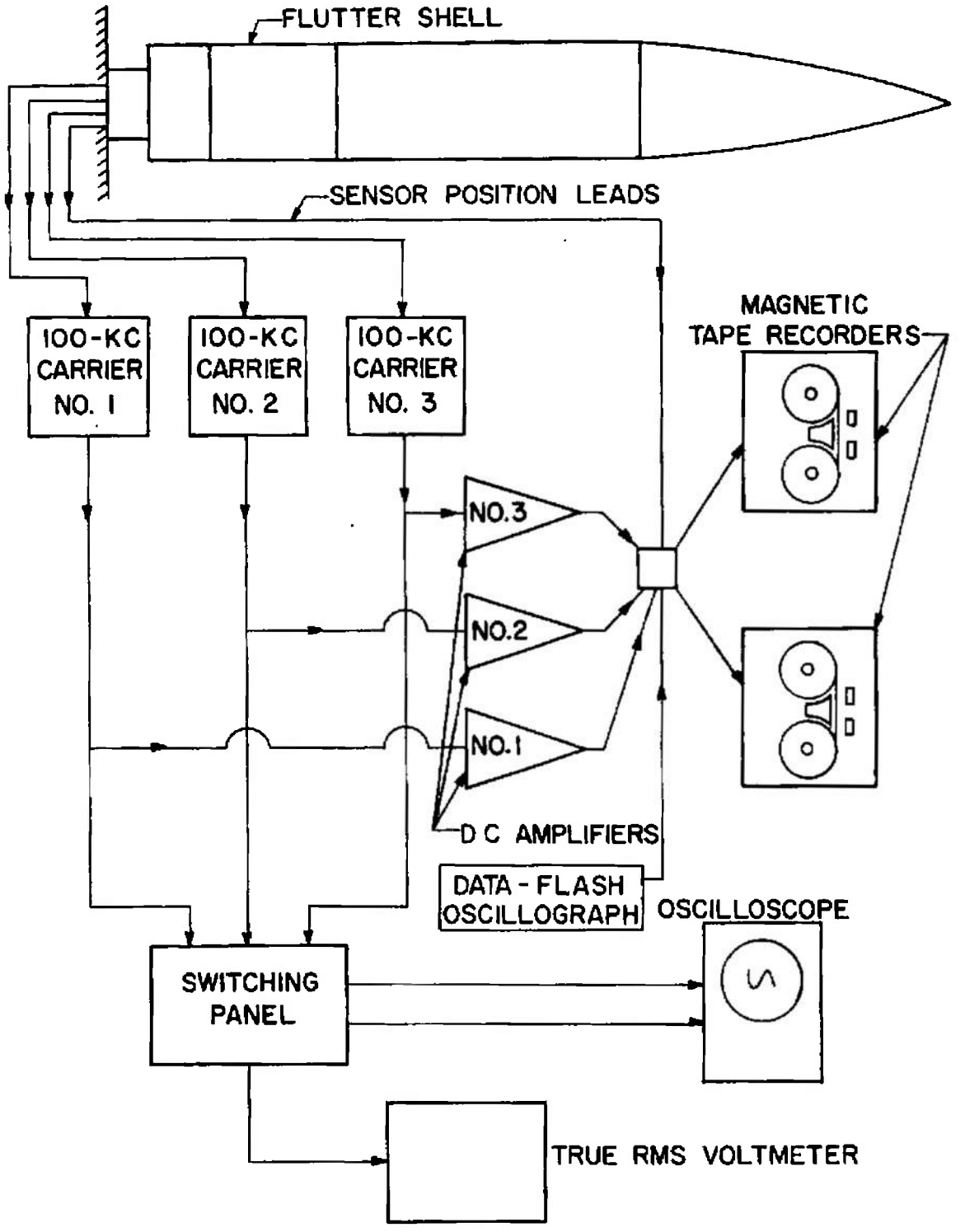

Fig. 10 Instrumentation Layout for Flutter Phase

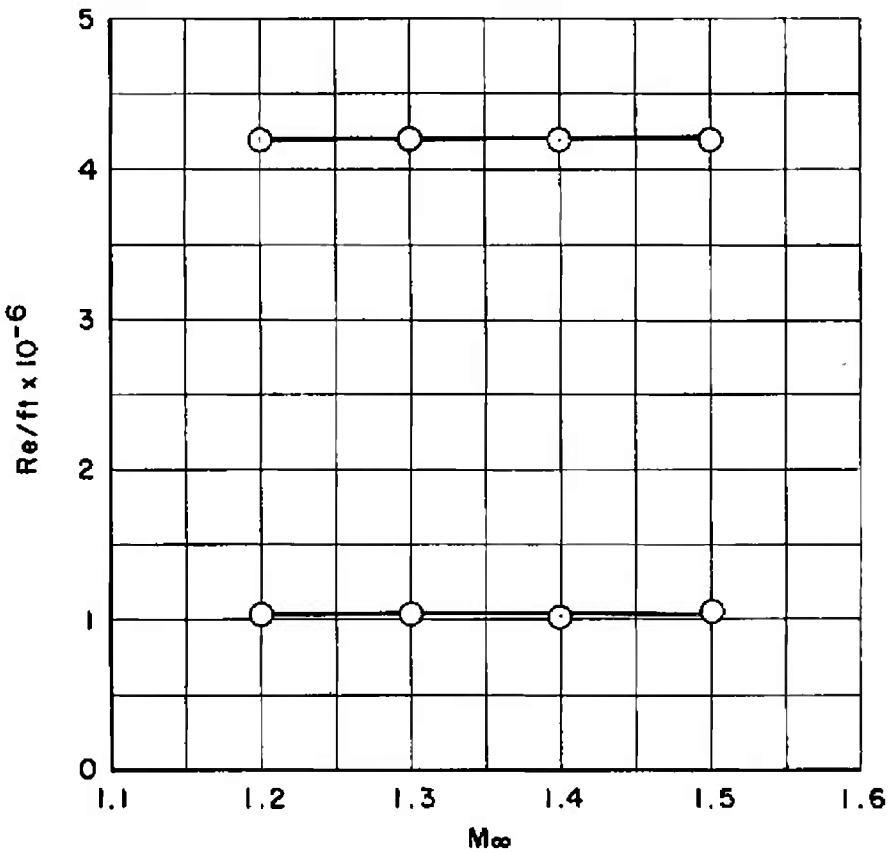

Fig. 11 Variation of Reynolds Number with Mach Number for Pressure Phase

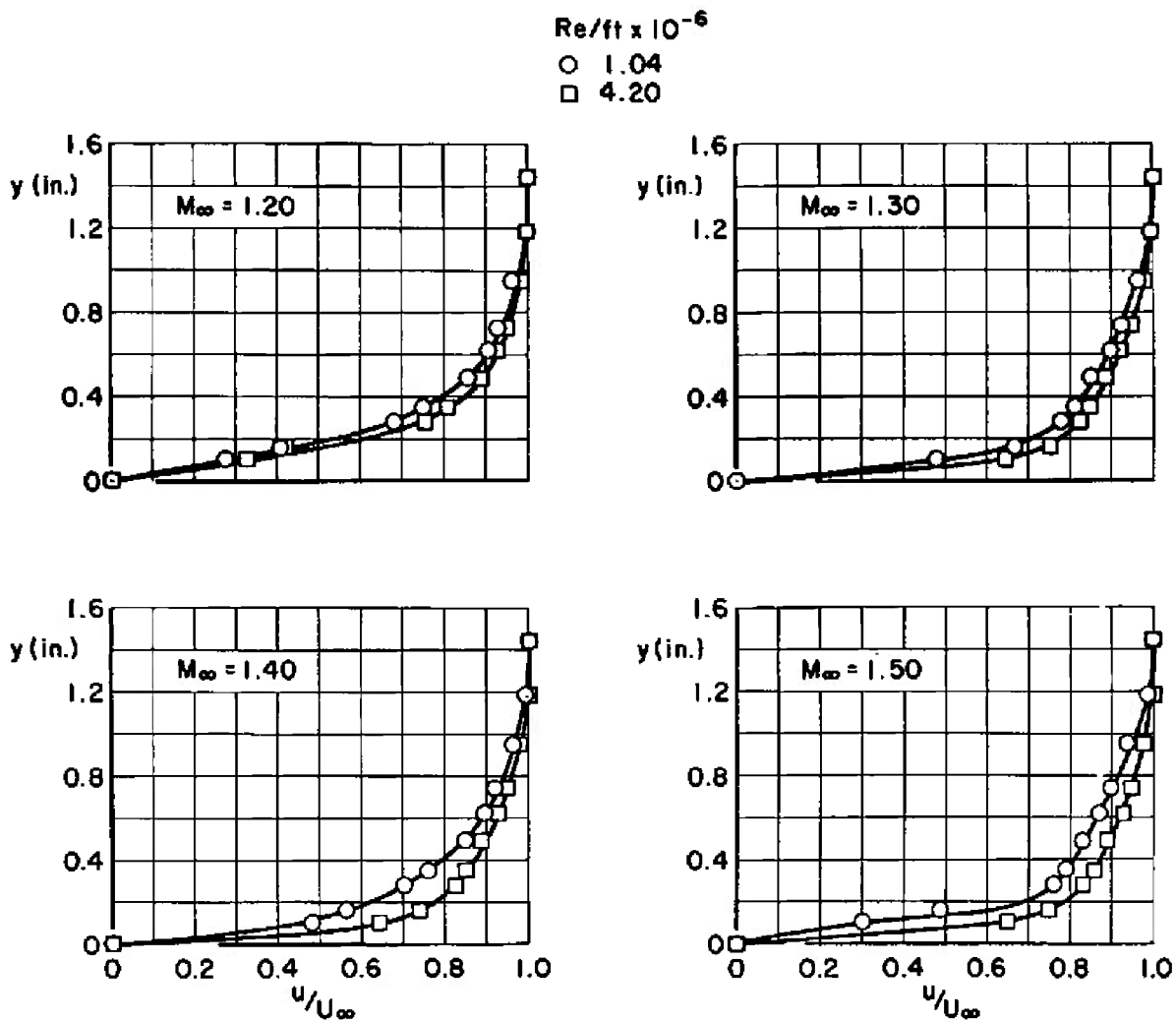

a. Reynolds Number Variation

Fig. 12 Boundary-Layer Profiles

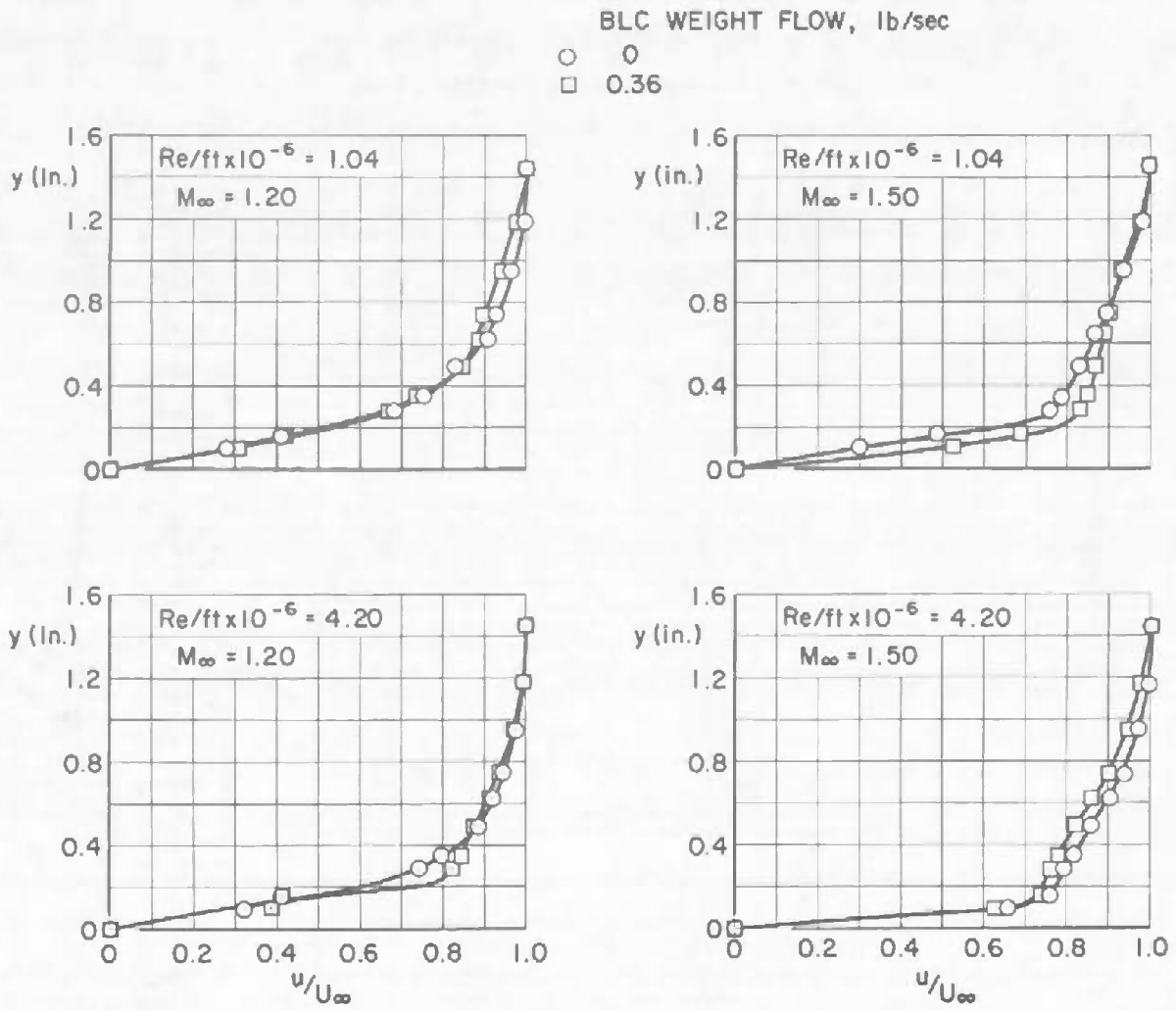

b. BLC Variation

Fig. 12 Concluded

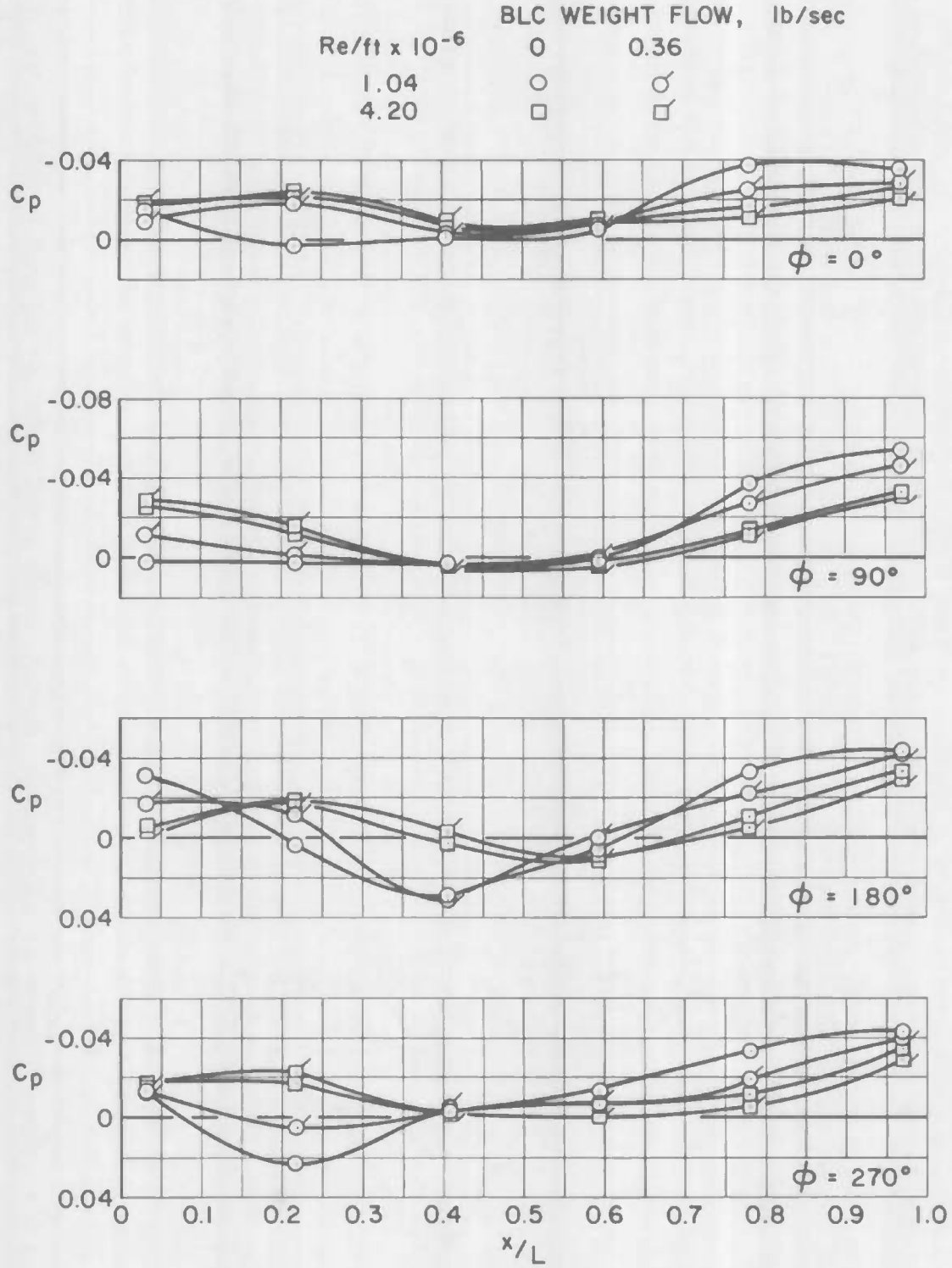

a. $M_\infty = 1.20$

Fig. 13 Variation of Pressure Coefficient along the Pressure Shell

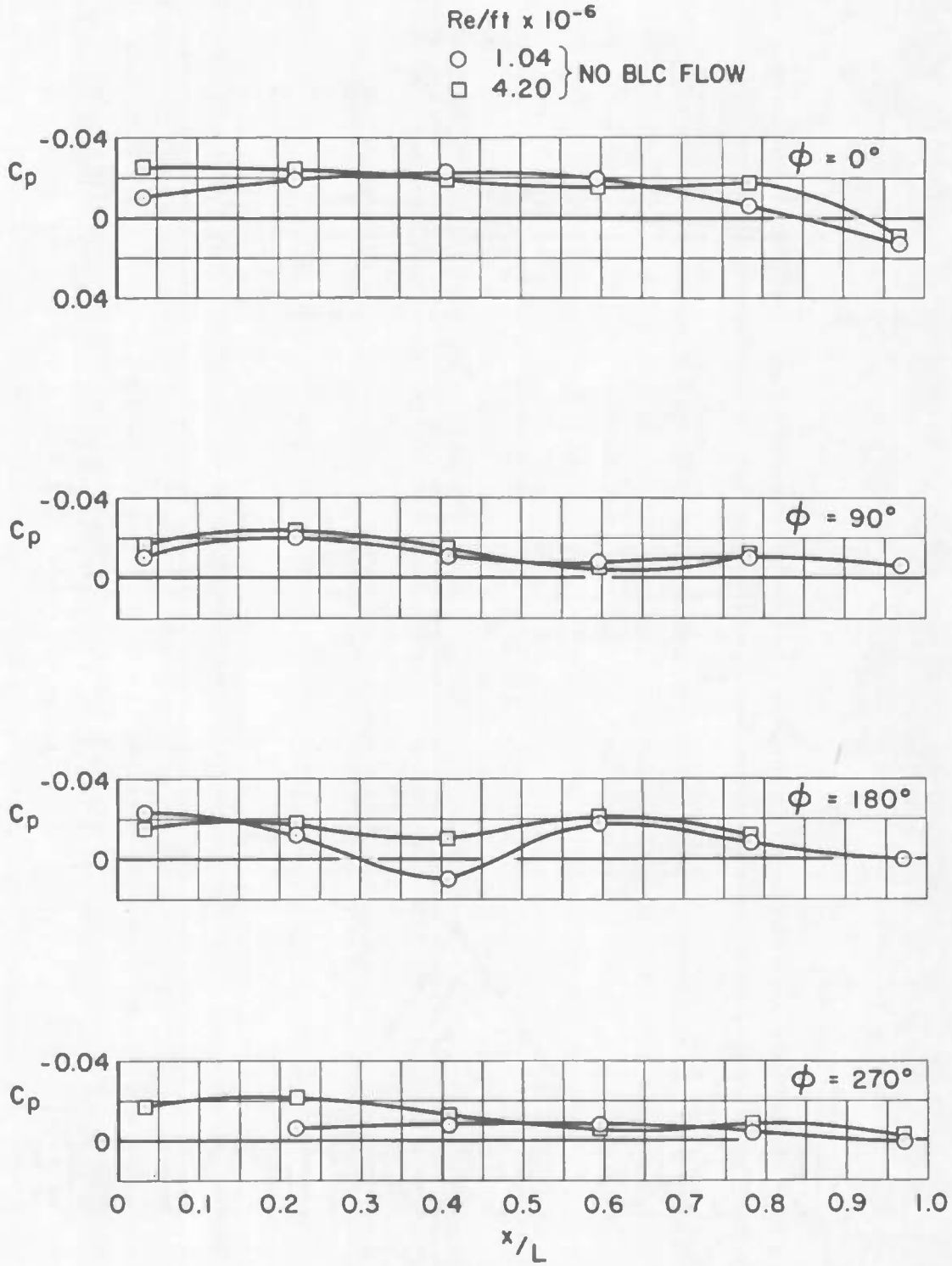

b. $M_\infty = 1.30$

Fig. 13 Continued

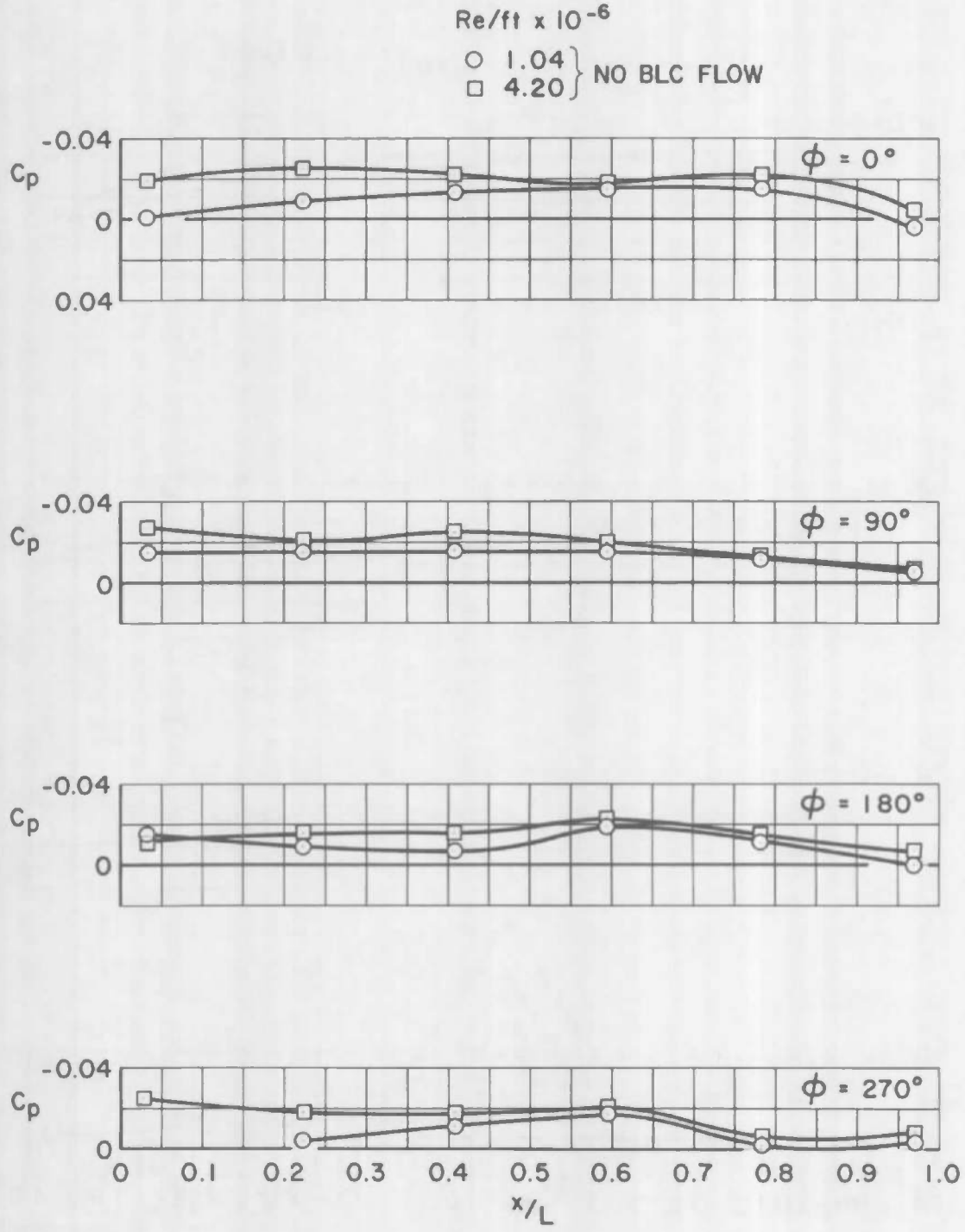

c. $M_\infty = 1.40$

Fig. 13 Continued

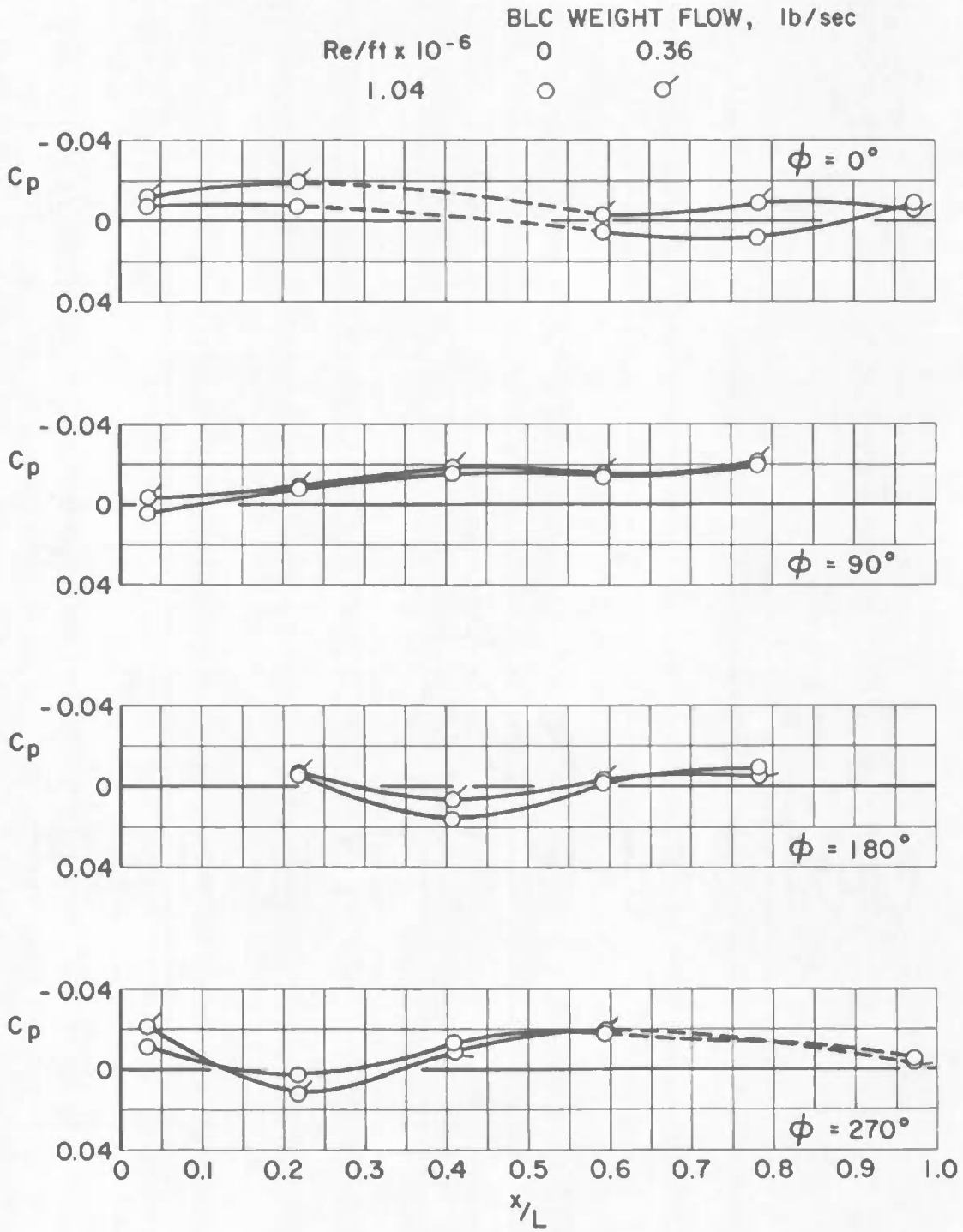

d. $M_\infty = 1.50$

Fig. 13 Concluded

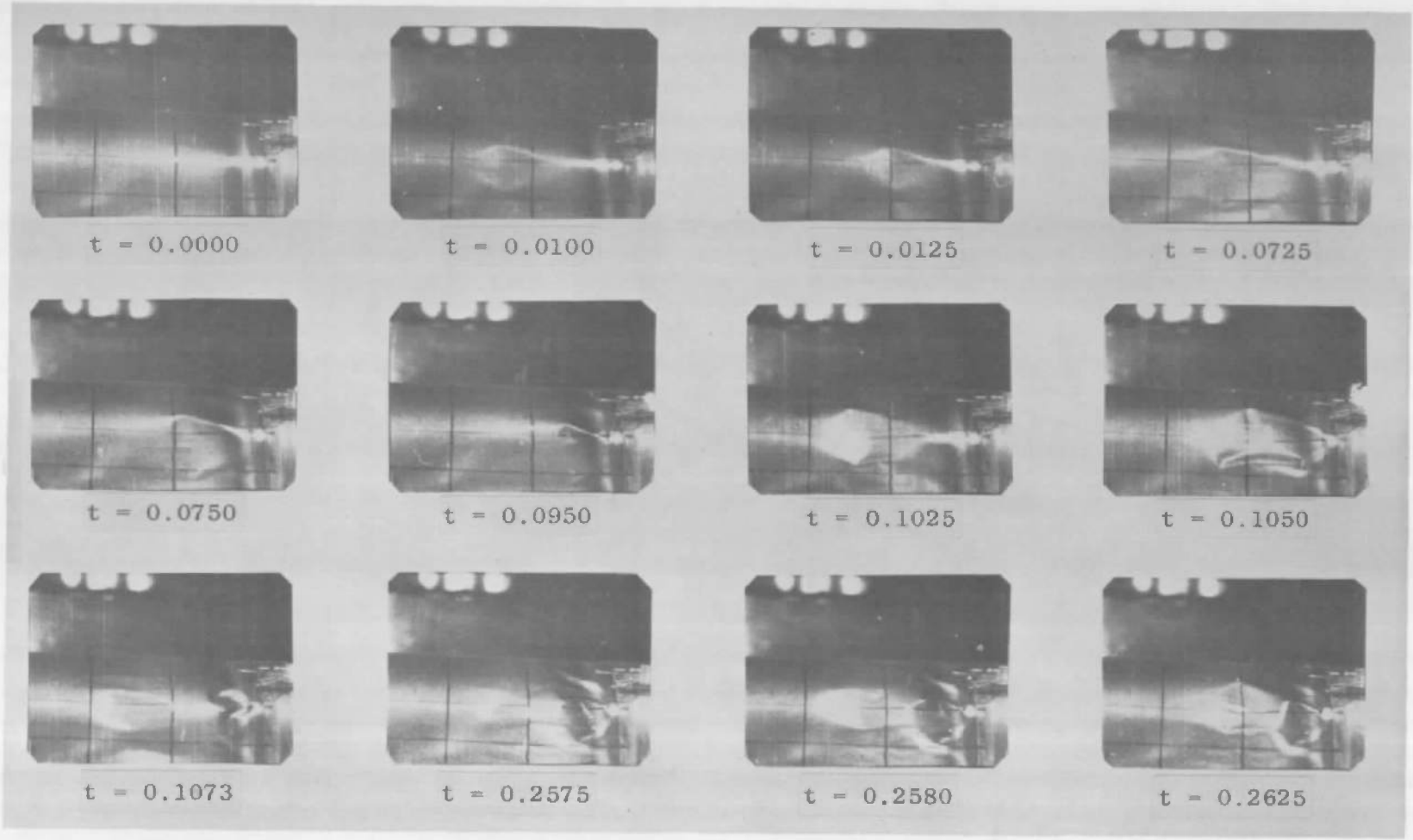

a. Longitudinal Traveling Wave

Fig. 14 Sequence from High Speed 16-mm Motion-Picture Film Illustrating Shell Failure

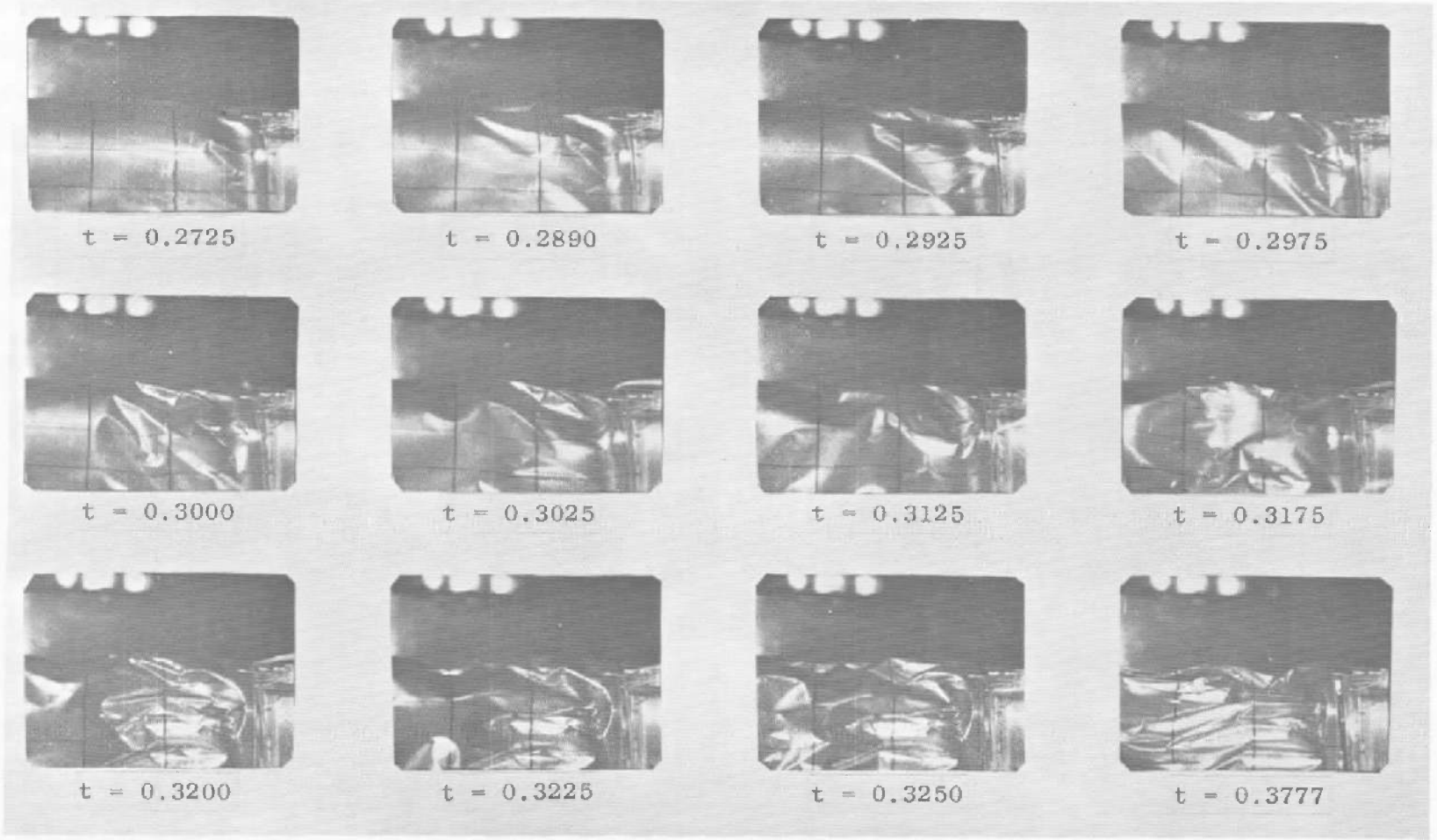

b. Circumferential Traveling Wave and Shell Failure

Fig. 14 Concluded

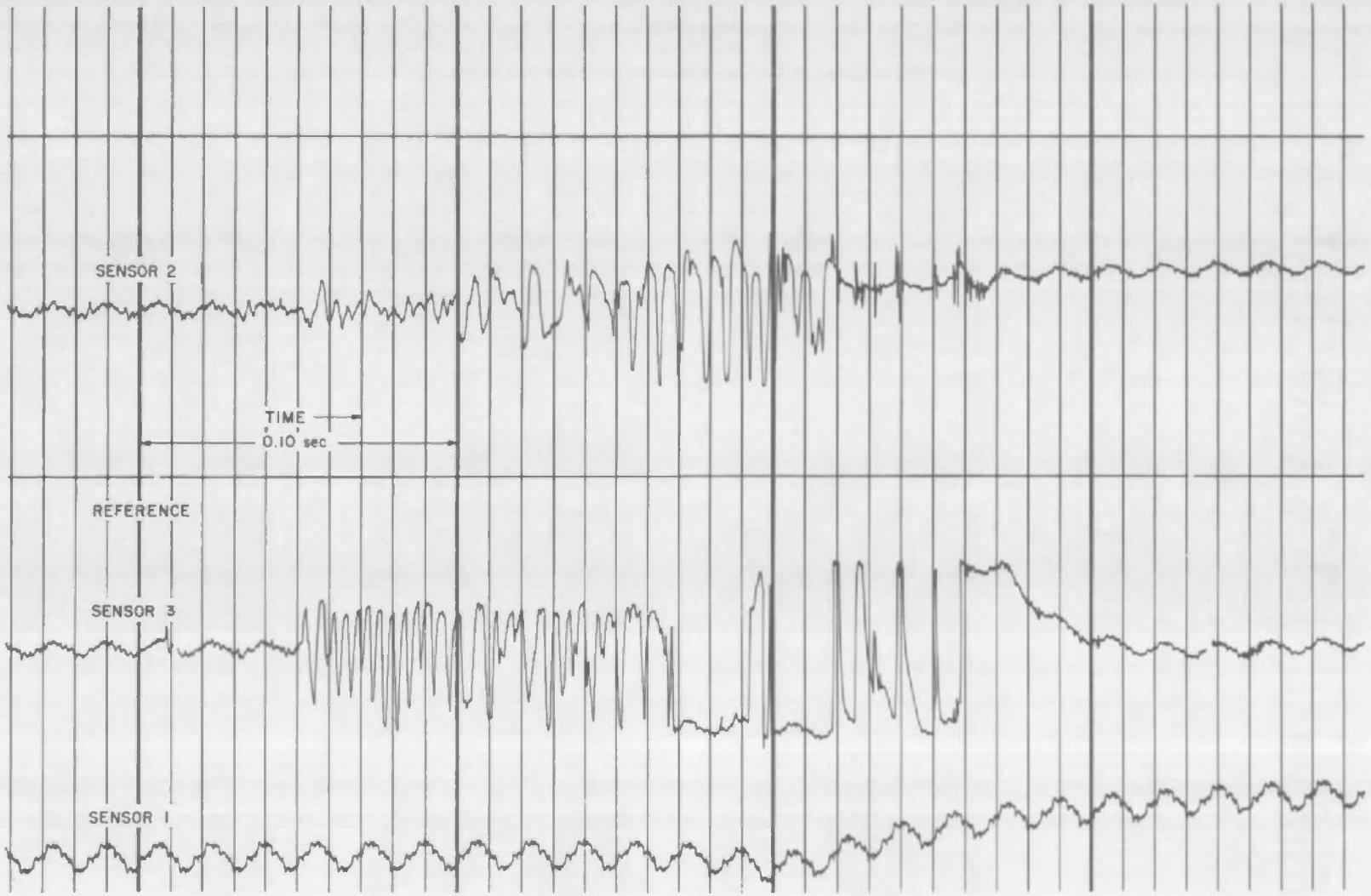

Fig. 15 Oscillograph Trace Showing Divergent Flutter

TABLE I
SUMMARY OF FLUTTER PHASE RESULTS

CONFIGURATION			M_∞	p_{t_∞}, psf	q_∞, psf	Re/ ft x 10^{-6}	BLC Valve, percent open	Δp_c, psi	p_f, psi	p_g, psi	f, cycles/sec	n, in./sec	$\frac{R}{h}$	$\bar{F}$
No.	End-Fixity	h, in.												
1	FLOATING	0.0032	1.200	2600	1082	5.39	0	0 236	41.3	0	240	—	2500	23.28
2	FORWARD END FIXED	0.0020	1.500	2000	858	4.03	25	1.000	33.4	23.4	135	—	4000	29.00
3	BOTH ENDS FIXED	0.0032	1.200	2600	1081	5.39	0	0.754	45.7	0	150	540	2500	23.28
4	FORWARD END FIXED	0.0020	1.500	2000	857	4.02	0	0.440	56.4	23.4	145	520	4000	29.00
5	FORWARD END FIXED	0.0040	1.200	2600	1081	5.40	0	0.530	16.1	30.0	150	—	2000	18.63

DOCUMENT CONTROL DATA - R&D

(Security classification of title, body of abstract and indexing annotation must be entered when the overall report is classified)

1 ORIGINATING ACTIVITY (Corporate author) Arnold Engineering Development Center, ARO, Inc., Operating Contractor, Arnold Air Force Station, Tennessee	2a REPORT SECURITY CLASSIFICATION UNCLASSIFIED 2b GROUP N/A

3 REPORT TITLE

AN INVESTIGATION OF THE AEROELASTIC STABILITY OF THIN CYLINDRICAL SHELLS AT TRANSONIC MACH NUMBERS

4 DESCRIPTIVE NOTES (Type of report and inclusive dates)

N/A

5 AUTHOR(S) (Last name, first name, initial)

Perkins, T. M., and Brice, T. R., ARO, Inc.

6 REPORT DATE	7a TOTAL NO OF PAGES	7b NO OF REFS
May 1966	36	3

8a CONTRACT OR GRANT NO AF40(600)-1200	9a ORIGINATOR'S REPORT NUMBER(S)
b PROJECT NO. 7063	AEDC-TR-66-93
c Program Element 61445014	9b OTHER REPORT NO(S) (Any other numbers that may be assigned this report)
d	N/A

10 AVAILABILITY/LIMITATION NOTICES

Qualified users may obtain copies of this report from DDC, and distribution of this document in unlimited.

11 SUPPLEMENTARY NOTES	12 SPONSORING MILITARY ACTIVITY
N/A	Air Force Office of Scientific Research, Air Force Systems Command, Washington, D. C.

13 ABSTRACT

Static pressure and boundary-layer data were obtained over a rigid pressure shell at Mach numbers from 1.20 to 1.50 and Reynolds numbers from 1.04 to 4.20 x 10^6/ft in the 16-ft transonic tunnel. These data were obtained with and without addition of air into the boundary layer through a circular slot upstream of the test shell. Flutter characteristics of thin cylindrical shells were obtained at Mach numbers of 1.20 and 1.50 with and without boundary-layer blowing and shell axial loading. Spirally traveling waves appeared on three of the shells just prior to divergent flutter, which was initiated by reducing shell cavity pressure.

14 KEY WORDS	LINK A		LINK B		LINK C	
	ROLE	WT	ROLE	WT	ROLE	WT
cylindrical shells						
aeroelastic stability						
pressure phase						
flutter phase						
supersonic flow						

1. Thin shells
2. Cylindrical bodies --
3. " shells --
4. " " -- Flutter, Distribution
5.
6. " 17 Boundary layer.

INSTRUCTIONS

1. ORIGINATING ACTIVITY: Enter the name and address of the contractor, subcontractor, grantee, Department of Defense activity or other organization *(corporate author)* issuing the report.

2a. REPORT SECURITY CLASSIFICATION: Enter the overall security classification of the report. Indicate whether "Restricted Data" is included. Marking is to be in accordance with appropriate security regulations.

2b. GROUP: Automatic downgrading is specified in DoD Directive 5200.10 and Armed Forces Industrial Manual. Enter the group number. Also, when applicable, show that optional markings have been used for Group 3 and Group 4 as authorized

3. REPORT TITLE: Enter the complete report title in all capital letters. Titles in all cases should be unclassified. If a meaningful title cannot be selected without classification, show title classification in all capitals in parenthesis immediately following the title.

4. DESCRIPTIVE NOTES: If appropriate, enter the type of report, e.g., interim, progress, summary, annual, or final. Give the inclusive dates when a specific reporting period is covered.

5. AUTHOR(S): Enter the name(s) of author(s) as shown on or in the report. Enter last name, first name, middle initial. If military, show rank and branch of service. The name of the principal author is an absolute minimum requirement.

6. REPORT DATE: Enter the date of the report as day, month, year, or month, year. If more than one date appears on the report, use date of publication.

7a. TOTAL NUMBER OF PAGES: The total page count should follow normal pagination procedures, i.e., enter the number of pages containing information.

7b. NUMBER OF REFERENCES: Enter the total number of references cited in the report.

8a. CONTRACT OR GRANT NUMBER: If appropriate, enter the applicable number of the contract or grant under which the report was written.

8b, 8c, & 8d. PROJECT NUMBER: Enter the appropriate military department identification, such as project number, subproject number, system numbers, task number, etc.

9a. ORIGINATOR'S REPORT NUMBER(S): Enter the official report number by which the document will be identified and controlled by the originating activity. This number must be unique to this report.

9b. OTHER REPORT NUMBER(S): If the report has been assigned any other report numbers *(either by the originator or by the sponsor)*, also enter this number(s).

10. AVAILABILITY/LIMITATION NOTICES: Enter any limitations on further dissemination of the report, other than those imposed by security classification, using standard statements such as:

(1) "Qualified requesters may obtain copies of this report from DDC."

(2) "Foreign announcement and dissemination of this report by DDC is not authorized."

(3) "U. S. Government agencies may obtain copies of this report directly from DDC. Other qualified DDC users shall request through _____."

(4) "U. S. military agencies may obtain copies of this report directly from DDC. Other qualified users shall request through _____."

(5) "All distribution of this report is controlled. Qualified DDC users shall request through _____."

If the report has been furnished to the Office of Technical Services, Department of Commerce, for sale to the public, indicate this fact and enter the price, if known.

11. SUPPLEMENTARY NOTES: Use for additional explanatory notes.

12. SPONSORING MILITARY ACTIVITY: Enter the name of the departmental project office or laboratory sponsoring *(paying for)* the research and development. Include address.

13 ABSTRACT: Enter an abstract giving a brief and factual summary of the document indicative of the report, even though it may also appear elsewhere in the body of the technical report. If additional space is required, a continuation sheet shall be attached.

It is highly desirable that the abstract of classified reports be unclassified. Each paragraph of the abstract shall end with an indication of the military security classification of the information in the paragraph, represented as *(TS), (S), (C), or (U)*

There is no limitation on the length of the abstract. However, the suggested length is from 150 to 225 words.

14. KEY WORDS: Key words are technically meaningful terms or short phrases that characterize a report and may be used as index entries for cataloging the report. Key words must be selected so that no security classification is required. Identifiers, such as equipment model designation, trade name, military project code name, geographic location, may be used as key words but will be followed by an indication of technical context. The assignment of links, rules, and weights is optional.